

PERFORMANCE OF THE HIGH-ENERGY PION BEAM AT LAMPF

Richard D. Werbeck and Robert J. Macek
 Los Alamos Scientific Laboratory
 University of California
 Los Alamos, New Mexico 87544

Summary

The Los Alamos Clinton P. Anderson Meson Physics Facility (LAMPF) high-energy pion beam (P^3) is a three-bend channel with two achromatic output legs designed for high-intensity and moderate resolution. The best resolution was measured to be 0.2% in $\Delta p/p$. A phase space of about $25 \pi \text{ m}^2\text{-cm}$ is transmitted by the channel. A π^+ flux of 2×10^7 pions/s was measured for 300 MeV/c momentum when a $7 \mu\text{A}$ proton beam struck a 6 cm graphite target. Proton contamination for good quality π^+ beams up to 450 MeV is negligible when an energy degrader (graphite) is used to separate protons from pions. In actual operation, very little beam tuning is required. Focusing elements are set according to the TRANSPORT computer code. Additional rate and contamination data will be presented, as well as additional information gained from operating experience.

Purpose

The high-energy pion channel (P^3) at LAMPF is a flexible, general-purpose pion beam line capable of transmitting the highest energy pions that LAMPF can produce (~625 MeV kinetic energy). It is designed to give high-intensity pion beams (a maximum π^+ flux of $6 \times 10^9/\text{s}$) of moderate resolution (0.2% or larger), and it has built into it the flexibility required to meet the needs of a wide range of experimental requirements. The criteria for the design of the P^3 channel were primarily drawn from the requirements of the following classes of experiments:

- a. All experiments requiring pions with kinetic energies above 300 MeV,
- b. elementary particle physics experiments with pions, and
- c. nuclear physics and nuclear chemistry studies that can be made with a resolution of 0.2% or larger.

General Description and Design

The P^3 channel consists of three dipole and 16 quadrupole magnets, shown schematically in Fig. 1. It is basically a two-bend channel with a third bend that switches the beam between two spatially separated experimental areas.

The pion beam is produced by striking a production target (A-2) with the main proton beam. The target is shaped so that the horizontal projection that the channel views is minimized, to limit the horizontal source size for the beam line and to eliminate the possibility of correlations between the horizontal position of the proton beam and the horizontal position of the channel source; the vertical proton beam position on the production target is

critical in determining the vertical position of the channel source.

The channel optics are designed so that a dispersed double focus is formed at a point midway between the fourth and fifth quadrupoles. A variable momentum acceptance slit and a variable thickness graphite degrader for removing protons from the π^+ beams are located at this double focus. A second double focus is formed inside the third bending magnet. The pions and energy-degraded protons are spatially separated (by ~5 cm) at the second focus because of the second bending magnet; therefore, a movable proton absorber is placed just off the beam axis before the third bending magnet to remove protons from π^+ beams. The beam after the third bending magnet is designed to be achromatic; this magnet steers the beam into the appropriate experimental area. The two quadrupole doublets in each output leg are used to tune the pion beam phase space to the phase-space requirements of the experiment mounted in the experimental area.

Variable slits for changing the channel solid angle acceptance are located before and after the first bending magnet. To clean up the beam, variable slits

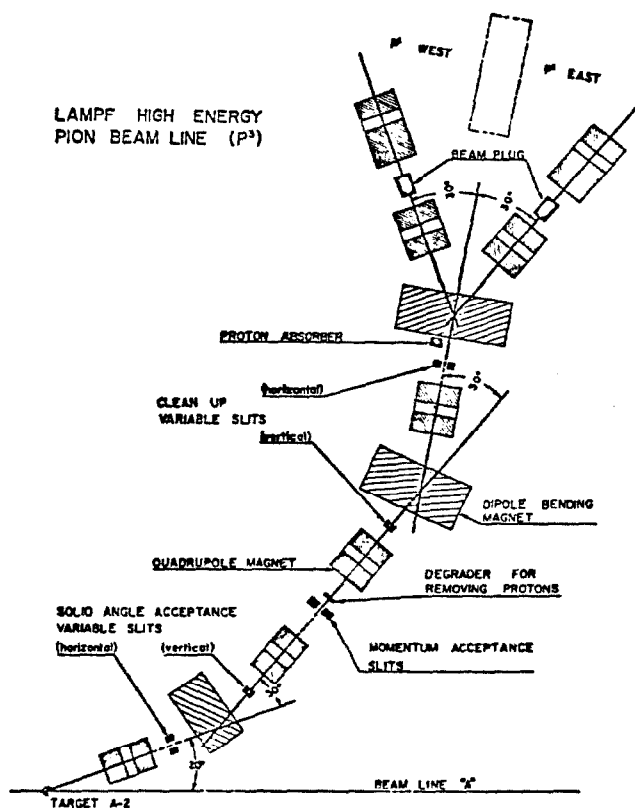


Fig. 1. Schematic of the LAMPF high-energy pion channel.

are located before the second bending magnet and before the third bending magnet; these slits are usually needed when the proton degrader, which multiply-scatters the pion beam, is used. Finally, movable beam plugs are located in each output leg of the channel.

This channel is further described in Ref. 1; more detailed channel design considerations, closely related to this design, are found in Ref. 2.

p³ Tune-Up

A sophisticated tune-up procedure that utilizes the pion beam transmitted by the channel was developed and employed to verify that the beam line was operating as designed. In particular, the phase space of the beam through the channel was measured and compared with the results predicted by computer codes. The criteria used to determine the quality of the channel tune were numerical values of error functions that were minimized in an on-line least-squares search. Details of the on-line tune-up of the channel may be found in Ref. 3, and the on-line optimization method employed in the tune-up procedure may be found in Ref. 4.

The solution of the magnet settings of the minimized optimizer function used in the tune-up procedure showed that all experimentally determined quadrupole magnet settings are in good agreement (within 2.3%) with those predicted by the computer code used in the design of the channel (TRANSPORT).^{5,6} Furthermore, the phase space measured through this experimental optimization was in good agreement with the predicted phase space.

In addition to the above tune-up of the channel, an alpha particle tune-up was performed to measure the best resolution of the section of the channel before the momentum slit. Finally, a considerable amount of beam time was used to obtain rate and beam composition data at different momenta for the channel.

Characteristics

Table I lists some of the most important characteristics of the p³ channel. Measured values of quantities, such as dispersion and resolution, are in good agreement with calculated values. It should be noted that when the channel is set up for maximum solid angle (a total momentum bite of 5%) and unity horizontal magnification, one obtains a second-order rms horizontal spot size of ±1.0 cm; the vertical size is ±0.8 cm. In this case, the second-order rms horizontal divergence is ±20 mr; the vertical divergence is ±25 mr.

Table II lists the π⁺ and π⁻ fluxes and beam composition as a function of pion momentum (kinetic energy) for a total momentum bite of 5% and the maximum solid angle when 1 mA of proton current strikes a 6 cm graphite target. These rates were obtained by measuring fluxes for smaller solid angle and momentum bite with about 10 μA of proton current on the target and extrapolating to the conditions outlined above. Rates were also calculated using production cross sections, channel solid angle, etc. The comparison of π⁻ rates between measured values and purely calculated values is shown in Fig. 2; the agreement is quite good.

TABLE I
CHARACTERISTICS OF THE HIGH-ENERGY PION BEAM AT LAMPF

Production Angle	20°
Two Achromatic Output Legs	
Total Length (to a point 0.9 m downstream of last output quadrupole)	19.5 m
Maximum Pion Momentum	-750 MeV/c
Maximum Pion Kinetic Energy	-625 MeV/c
Maximum Solid Angle (for 1% total momentum bite)	-7 msr
Maximum Total Momentum Bite	-13%
Best Resolution (for 0.5 cm long production target)	0.2%
Resolution for 6 cm long Production Target	1.6%
Dispersion: West Leg	1.8 cm/%Δp/p
East Leg	1.5 cm/%Δp/p
First-Order Phase Space: Horizontal	~22 π mr-cm
Vertical	~25 π mr-cm

TABLE II
PION FLUXES FROM P³ CHANNEL^a

Momentum (MeV/c)	Kinetic Energy (MeV)	π ⁺ Data ^b			π ⁻ Data ^d	
		π ⁺ /s (x 10 ⁹)	p/π ⁺ Ratio	π ⁺ /All ^c (No Protons)	π ⁻ /s (x 10 ⁸)	π ⁻ /All ^c
200	104	0.36	0.00	0.68	1.25	0.42
300	191	1.68	0.00	0.95	3.92	0.80
350	237	2.35	0.01	0.98	5.04	0.91
400	284	3.15	0.02	0.996	5.59	0.976
450	332	3.43	0.04	0.999	4.91	0.990
500	380	2.76	0.09	1.000	3.36	1.000
600	476	0.70	0.65	1.000	0.72	1.000
700	574	0.04	18.9	1.000	0.03	1.000

^ap³ fluxes for the following conditions: (1) maximum solid angle of channel, -7 msr, (2) total momentum bite, Δp/p = 5%, and (3) 1 mA proton current on 6 cm graphite target.

^bπ⁺ data obtained using enough graphite degrader in p³ at each momentum to give ~9.5 mr multiple scattering to π⁺.

^cAll implies the nonproton part of the beam = π + μ + e.

^dπ⁻ data obtained using no degrader.

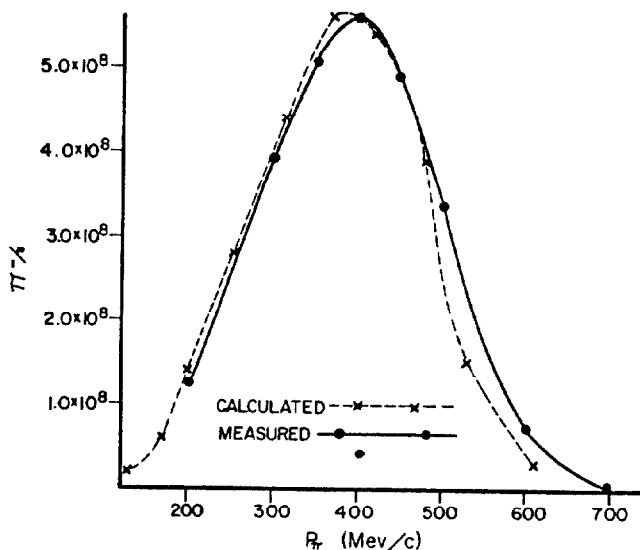


Fig. 2. Comparison of measured vs calculated π⁻ rates for the P³ channel.

Operation and Performance

In actual beam line operation, the beam travels through a vacuum. All beam line components are remotely operable, and computer control of all magnets and variable slits will be implemented in the near future.

The P^3 channel at LAMPF has been in operation for about 16 months. The last 9 months of operating time were devoted to experiments; the channel has run quite reliably during this time. Table III shows a listing of the experiments that have received beam time on the channel, the number of shifts of beam received, and the actual number of $\mu\text{A}\cdot\text{h}$ of proton current on the A-2 target delivered for each experiment. Most experiments have not been completed, and will return when high-intensity operation is a reality.

TABLE III

EXPERIMENTS PERFORMED ON LAMPF HIGH-ENERGY PION CHANNEL

	Shifts	$\mu\text{A}\cdot\text{h}$ (k)
Pion Beta Decay (Temple University/LASL)	79	2.7
Elastic Scattering of Pions from Deuteron (University of Virginia)	79	4.2
Forward Elastic Scattering of Pions from Different Targets (Rice University)	63	1.1
Time-Reversal-Invariance Test in Single Pion Photoproduction Through a Study of Reciprocity in the Reactions of Pions on ^3He and T (UCLA/LASL)	9	0.5
Cross-Section Measurement for $\pi^- p \rightarrow \pi^+ \pi^-$ (University of Wyoming/LASL/Colorado College)	55	3.1
Interaction of Stopped Negative Pions with Complex Nuclei (Argonne National Laboratory)	6	0.3
Study of Nuclear Gamma Rays from In-Flight π and p Reactions (CMI)	2	0.1
Nuclear Chemistry (four) (mostly LASL)	39	1.6

References

1. P^3 Users Group and P. A. M. Gram, "A Proposal for P^3 , a Versatile High-Energy Pion Beam Facility," Los Alamos Scientific Laboratory report LA-4535-MS (September 1970).
2. R. J. Macek, "Preliminary Report on Some General Purpose Two-Bend Pion Channels," Los Alamos Scientific Laboratory internal document MP6/RJM-1 (April 1970); R. J. Macek, Addendum I, "A Multiplexed P^3 Channel" (1970).
3. N. D. Gabitzsch, D. Mann, G. Pfeufer, C. C. Phillips, J. Hudomalj, L. Y. Lee, M. Warneke, J. C. Allred, R. J. Macek, and R. D. Werbeck, "Tune Up of the LAMPF High-Energy Pion Channel," Nucl. Instr. & Methods (to be published).
4. J. Hudomalj, D. Mann, N. D. Gabitzsch, C. Bordner, and R. J. Macek, "A Computational Technique for Tuning the LAMPF High-Energy Pion Channel," Nucl. Instr. & Methods (to be published).
5. Karl L. Brown, "A First- and Second-Order Matrix Theory for the Design of Beam Transport Systems and Charged Particle Spectrometers," Stanford Linear Accelerator Center report SLAC-75, Revised, UC-28 (May 1969).
6. Karl L. Brown, Sam K. Howry, "TRANSPORT/360, A Computer Program for Designing Charged Particle Beam Transport Systems," Stanford Linear Accelerator Center report SLAC-91, UC-28 (EXPI) & (ACC) (July 1970).

It should be noted that π^+ rates and proton contamination were determined using enough graphite degrader at each momentum to give ~ 9.5 mr multiple scattering to the pions in the beam. As one increases the degrader thickness that is used to remove protons, both the proton contamination to the pion beam (because of increased energy degradation to the protons) and the pion flux (because of increased multiple scattering to the pions) are reduced. Figure 3 shows how the π^+ flux is affected by using different degrader thicknesses, resulting in different amounts of multiple scattering to the π^+ beam; the relative flux for 350 MeV/c π^+ shown in this graph is the ratio of the π^+ flux for any given pion multiple scattering to the π^+ flux for a pion multiple scattering of 4.5 mr. Figure 4 shows how the proton contamination to the pion beam varies as a function of pion multiple scattering for a 625 MeV/c π^+ beam. With no degrader material in the beam (i.e., no multiple scattering to the pions), one expects about 100 times as many protons as pions in the beam.

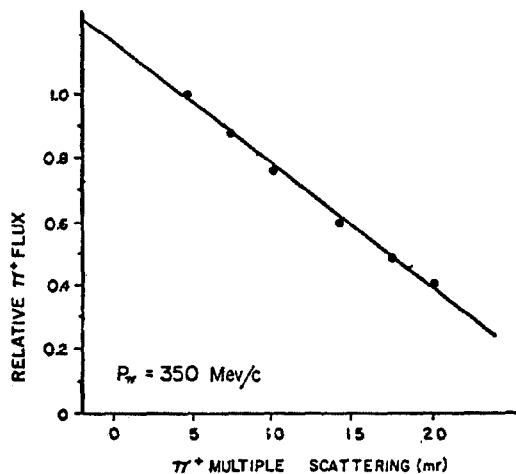


Fig. 3. Relative changes in pion flux intensity due to the insertion of different amounts of proton degrader material in the beam.

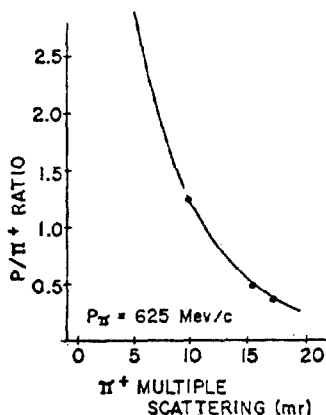


Fig. 4. Relative changes in proton contamination to the π^+ beam due to the insertion of different amounts of proton degrader material.